Chem Soc Rev

Cite this: *Chem. Soc. Rev.*, 2012, **41**, 7464–7478

www.rsc.org/csr

CRITICAL REVIEW

Magnetic polyoxometalates: from molecular magnetism to molecular spintronics and quantum computing†

Juan M. Clemente-Juan, Eugenio Coronado* and Alejandro Gaita-Ariño

Received 7th June 2012
DOI: 10.1039/c2cs35205b

In this review we discuss the relevance of polyoxometalate (POM) chemistry to provide model objects in molecular magnetism. We present several potential applications in nanomagnetism, in particular, in molecular spintronics and quantum computing.

1. Introduction

Spin-based electronics (or spintronics) is one of the emerging branches in nanotechnology and the most active area within nanomagnetism. Its central subject is the active manipulation of spin degrees of freedom of charge carriers in solid-state systems, in addition to their electronic charge used in traditional semiconductor electronics. The field has made a major impact on today's daily life, for instance, by improving hard drive information storage and in magnetic sensing. The range of applications of spintronics is now expanding from read-heads devices, to new types of non-volatile magnetic memories (MRAM),[1,2] to spin transfer nano-oscillators for applications in future wireless telecommunications,[3] to the potential use of an individual electron spin system as a quantum bit in a quantum computer.[4]

Instituto de Ciencia Molecular (ICMol), Universidad de Valencia, C/ Catedrático José Beltrán, 2, E-46980 Paterna, Spain. E-mail: eugenio.coronado@uv.es
† Part of a themed issue covering the latest developments in polyoxometalate science.

Up to now, "conventional" spintronics has been almost exclusively based on inorganic metals and semiconductors.[5,6] However, with the contemporary evolution of molecular electronics and molecular magnetism, and with the evolution of spintronics towards nanospintronics, a new field namely *Molecular Spintronics* is emerging that combines the ideas and concepts developed in spintronics with the unique possibilities offered by the molecular systems to perform electronic functions, to form self-organized nanostructures and to exhibit quantum effects at the nanoscale.[7,8] This new field can take advantage of the possibilities offered by molecular electronics in the materials processing, as well as in the manipulation, measurement and addressing of individual molecules, and by the molecular magnetism in the increasing control over the chemical design of magnetic molecules and materials with desired properties. A standing challenge in molecular spintronics is the preparation of complex functional circuits, because Nature tends to prefer periodic structures such as crystals. Possible solutions include profiting from solid state technology by binding molecules to surface nanopatterns, adopting a cellular automaton strategy by using molecules which

Juan M. Clemente-Juan

Juan M. Clemente-Juan received his PhD in Chemistry in 1998 at the Universidad de Valencia under the supervision of Prof. E. Coronado and Dr J. J. Borras-Almenar. From 1998 to 2001 he was a post-doctoral researcher in the group of Prof. J. P. Tuchagues. Since 2001 he has been a researcher at ICMol (Universidad de Valencia). His research interests cover different aspects of molecular magnetism: exchange-coupled and single ion SMM and mixed valence systems.

Eugenio Coronado

Eugenio Coronado has been Professor of Inorganic Chemistry at the University of Valencia since 1993 and Director of the University's Institute of Molecular Science (ICMol) since its foundation in 2000. He is the author of numerous contributions in molecular magnetism, with particular emphasis on the chemistry and physics of multifunctional molecular materials and nanomagnets. Currently, his research is focused on the use of these magnetic materials in molecular spintronics.

individually offer complex functionality or taking clues from biology and advancing in the dynamic science of structure, form and function.

An important breakthrough in molecular magnetism that has contributed to this evolution has been the discovery of single-molecule magnets *i.e.*, magnetic molecules showing slow relaxation of the magnetization at low temperatures and quantum effects.[9] Owing to these distinctive properties, SMMs have been proposed as useful molecular objects for molecular spintronics.[10] Other interesting features of the molecular world come from its chemical, structural and electronic versatilities. Thus, in organic systems electron spins can be preserved for longer periods of time and distances than in conventional inorganic materials.[11] On the other hand, the spin-relaxation times of magnetic molecules can be exceptionally long – between a few milliseconds and seconds.[12] Finally, the low-density, flexibility, transparency, processability, ability of self-assembling, and novel added functionalities (magnetic switching at the molecular level, emission of light, *etc.*) of the molecular systems can also justify this interest.

In a similar way to what happens in molecular electronics, molecular spintronics can be divided into two large sub-areas named "molecule-based spintronics" and "unimolecular spintronics". The first focuses on the design and study of new molecule-based materials that can mimic the properties of the existing inorganic (spin)-electronic materials/structures/devices or even improve them. It opens the possibility to design cheaper spintronic devices compatible with plastic technology.[13] The second is devoted to the study of individual magnetic molecules as active components of nanospintronic devices (including ultra-high density information-storage devices). It takes advantage of the possibility to chemically tailor molecules with control down to the single spin for the construction of ultra small spintronic devices[14] with the perspective of using these magnetic molecules as qubits for quantum computing.

Very recently, the first steps in the manipulation of molecular spin instead of its charge have been undertaken, revealing tentative potential for memory or quantum information technology. This novel approach should enable the creation of electrically addressable single-molecule magnetic qubits and molecular switches.[15] It is time to explore the potential of POMs in this context since, when compared with other coordination compounds, these molecular-metal oxides present some advantageous chemical, structural and electronic features that make them suitable for this goal, namely:

(i) They are robust molecules that keep their integrity in the solid state, in solution and probably also on surfaces.

(ii) They can accommodate magnetic ions or groups of magnetic ions at specific sites of the rigid POM structure, leading to magnetic molecules and large magnetic clusters with specific topologies and highly symmetric environments.

(iii) They can accept various numbers of electrons, while keeping almost intact their structure, leading to mixed-valence systems in which the extra electrons are extensively delocalized over the whole POM framework.

In this review we will discuss the relevance of polyoxometalate (POM) chemistry in nanomagnetism and, in particular, in molecular spintronics and quantum computing. Traditionally, the most extended application of these molecular-metal oxides deals with catalysis. Still, owing to their structural and electronic versatilities, we already pointed out in the 1990's that POMs could also be model objects in molecular magnetism, or magnetic components of hybrid molecular materials.[16–18] Nowadays, these trends have expanded towards nanomagnetism. These recent advances will be presented in the first part of the review, where we will focus in particular on the recent discovery of lanthanide single-molecule magnets. Such a discovery has been seminal for the use of these nanomagnets in molecular spintronics and quantum computing. These new applications of POMs will be discussed in the second part of the review.

2. Relevance of POMs in molecular magnetism

2.1. Historical background: POMs as magnetic models

Until very recently the relevance of POMs in molecular magnetism was based on the ability of these molecular metal-oxides to provide ideal examples for studying at the molecular level the two key processes occurring in the extended structures formed by metal-oxide materials, namely magnetic exchange and electron delocalization. Two classes of magnetic POMs are of interest in this context namely the spin-localized POMs and the spin-delocalized mixed-valence (MV) POMs.

Spin-localized POMs. In these POMs the magnetic moments remain localized on the 3d or 4f magnetic metal ions. To prepare these systems we have benefited from the ability of heteropolyoxometalates, essentially wolframates and, to a lesser extent, molybdates, to act as chelating ligands toward practically all 3d-transition and/or 4f lanthanoid metal ions. This has afforded the encapsulation of these magnetic ions at specific sites of the framework structures, thus creating well-defined magnetic entities formed either by a single magnetic center or by various magnetic centers connected though oxo-bridges (magnetic clusters). Owing to the rigidity of these POM ligands, specific coordination geometries and nuclearities of the magnetic entities have been obtained leading, in

Alejandro Gaita-Ariño

Alejandro Gaita-Ariño received his PhD (2004) from the University of Valencia. After the completion of his PhD, he made short postdoctoral stays at the IRSAMC in the UPS in Toulouse, France and with Daniel Loss of the University of Basel in Switzerland. He worked as a postdoctoral researcher in the UBC, under the supervision of Philip C. E. Stamp. His main field of research is molecular magnetism. His current interests include spin qubits based on lanthanoid single-ion magnets and the universal low temperature properties in disordered and amorphous solids.

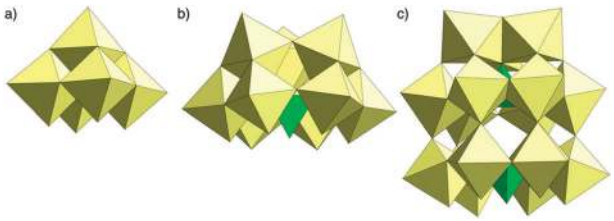

Fig. 1 Monovacant and trivacant ligands derived from Lindqvist, Keggin and Dawson–Wells structures: (a) $[W_5O_{18}]^{6-}$, (b) β-$[PW_9O_{34}]^{9-}$ and (c) $[P_2W_{15}O_{56}]^{12-}$.

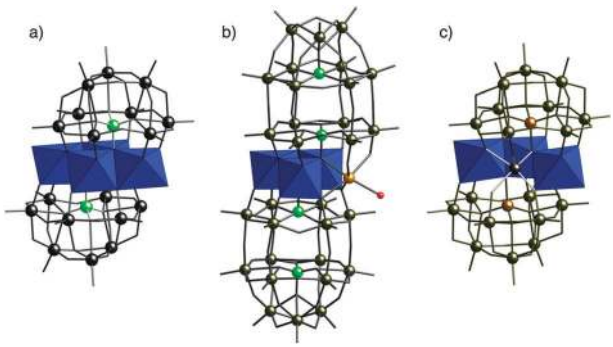

Fig. 2 Structures of the (a) $[Co_4(H_2O)_2(PW_9O_{34})_2]^{10-}$, (b) $[(NaOH_2)Co_3(H_2O)(P_2W_{15}O_{56})_2]^{17-}$ and (c) $[Co_3W(H_2O)(ZnW_9O_{34})_2]^{12-}$ clusters.

general, to extensive families of compounds in which these magnetic metal ions can be changed at will, while keeping practically unchanged the structural features of the magnetic entities. This ability has been exploited in particular in the so-called lacunary POMs, which are capped structures obtained by removal of part of the octahedral sites from the initial POM structure (Fig. 1). The literature offers an extensive number of examples of these magnetic clusters.[18,19]

In addition to the wide variety of paramagnetic cations that can be encapsulated, another advantageous feature has been the effective magnetic isolation guaranteed by the bulky non-magnetic POM framework, with typical distances between the magnetic ions of the order of 1–2 nm. Furthermore, clusters of higher nuclearity can be constructed from smaller fragments by controlling certain chemical parameters (stoichiometry, pH,...). This feature allows us to control not only the nuclearity but also the type of magnetic interactions between the different ions and thus stabilize a desired spin ground state.

All these features have made these complexes ideal candidates for modeling the magnetic exchange interactions in clusters of increasing nuclearities and definite topologies. During the last two decades a large number of highly symmetric clusters with intermediate nuclearities, such as dimers, trimers and tetramers, have been widely studied as model systems for the development of magnetic exchange theories.[18]

A relevant case that illustrates the possibilities offered by POM chemistry to conduct detailed studies on magnetic exchange interactions is provided by the cobalt(II) clusters. This d^7 ion, when octahedrally coordinated by the weak ligand field of POMs, shows a high-spin $S = 3/2$ with an unquenched orbital momentum, thus exhibiting a large spin anisotropy.[20] In fact, the first order spin–orbit coupling results in an effective and highly anisotropic spin doublet, $S = 1/2$. Still, the magnetic properties in these compounds have been shown to be largely insensitive to the exchange anisotropy and thus, other physical techniques have been used to extract this information. The key technique in this context has been Inelastic Neutron Scattering (INS). This spectroscopic technique provides a direct access to the splitting of the low-lying energy levels of a cluster caused by exchange interactions. Therefore, it allows a much deeper and more detailed insight into the nature of the magnetic coupling compared with the usual magnetic susceptometry.

In 1992 we started to use this technique to study a tetranuclear rhomb-like Co(II) cluster encapsulated by lacunary POMs of formula $[Co_4(H_2O)_2(PW_9O_{34})_2]^{10-}$ (see Fig. 2a).[21] These studies provided for the first time direct evidence about the Co(II)–Co(II) exchange anisotropy.[22] More recently we have shown that INS data are sensitive not only to the magnitude and anisotropy of the exchange parameters but also to the relative orientation of the exchange anisotropy axes. An illustrative example has been provided by studying two closely related trinuclear Co(II) clusters derived from the tetranuclear rhomb-like Co(II) cluster.[23] The first trimer is an angular Co_3 cluster obtained by replacement of a Co situated in the short diagonal of the rhomb by W (shorthand Co_3W) (Fig. 2c). It has been isolated in the POM salt $Na_{12}[Co_3W(H_2O)(ZnW_9O_{34})_2]\cdot nH_2O$. The second trimer is a triangular Co_3 cluster obtained by replacement of a Co placed in the long diagonal of the rhomb by Na^+ (shorthand $NaCo_3$) (Fig. 2b). It has been isolated in the POM salt $Na_{17}[(NaOH_2)Co_3(H_2O)(P_2W_{15}O_{56})_2]\cdot nH_2O$. The INS spectra of Co_3W show three cold peaks and three hot ones, while $NaCo_3$ shows up to two cold peaks and two hot peaks (Fig. 3, left).[24] From these data an energy splitting pattern can be obtained (Fig. 3, right). The diagrams show four doublets arising from the three coupled effective spins $S = 1/2$. These results have been closely reproduced by using a fully anisotropic exchange model that takes into consideration the molecular symmetry of the system. In this anisotropic model, the orientation of the local anisotropy axes is assumed to be parallel to the W–O bonds, and the three components (x, y and z) of each exchange interaction are different. Making use of the molecular symmetry of the cluster, it has been possible to describe the INS spectra of both systems from a set of 5 parameters, which are the following: (i) the three components of the exchange parameters $J^{13}{}_{(x,y,z)}$ associated with the side of the rhombus (similar for both clusters) and (ii) the two components of the axial exchange $J^{23}{}_{(x,y,z)}$ through the short diagonal ($J^{23}{}_x = J^{23}{}_y$ due to the C_s symmetry). In conclusion, the possibility of studying these Co clusters through INS has provided the opportunity to demonstrate for the first time in a direct way the anisotropic nature of the exchange interactions in magnetic clusters formed by this anisotropic metal ion.[23]

Mixed-valence POMs. To prepare these compounds one takes advantage of the electron acceptor ability of these metal-oxide clusters, by which a variable number of electrons can undergo a rapid electron transfer from one center to the other of the POM framework. This feature shows that POMs

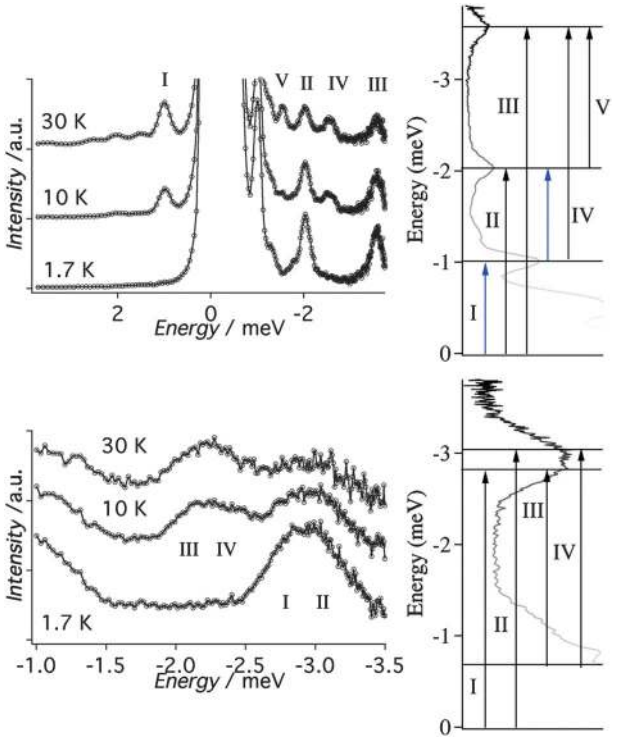

Fig. 3 INS spectra of polycrystalline sodium salts of $[Co_3W(H_2O)(ZnW_9O_{34})_2]^{12-}$ (top) and $[(NaOH_2)Co_3(H_2O)(P_2W_{15}O_{56})_2]^{17-}$ (bottom) clusters and experimentally determined ground-state splitting with observed transitions represented by arrows.

provide unique examples in coordination chemistry of high-nuclearity MV clusters. These spin-delocalized clusters represent a formidable challenge in molecular magnetism since their electronic complexity is much higher than that encountered in the spin-localized magnetic clusters. In fact, apart from the magnetic superexchange J, three additional processes need to be taken into account to model their properties, namely:

- Electron transfer, t, between adjacent "occupied" and "empty" sites, *i.e.* between two metals with different oxidation states (W(V)–W(VI); Mo(V)–Mo(VI); V(IV)–V(V)), which tends to delocalize the electron over the cluster.
- Coulombic repulsion, V, between every pair of electrons, which tends to place the electrons as far as possible to minimize its repulsion.
- Vibronic coupling, λ, that couples the "blue" electrons with the vibrational modes of the cluster, tending to localize the electron on a given site.

In addition, the unique ability of POMs to act as electron sponges hosting a variable number of electrons in the POM framework can provide an efficient way to tune the strength of the exchange coupling as well as the electron delocalization in the cluster and, consequently, its spin state. Such a control can be achieved either physically, by an electrical gating in a single-molecule setup, or chemically, during the synthesis of the POM. As we will see later on, this feature will be quite interesting in spintronics as it is expected to afford the control of the spin state of the cluster by applying an electric field.

A classic example of diamagnetic MV POM is provided by the anion $[PW_{12}O_{40}]^{5-}$, which is reduced by two electrons. The diamagnetism of this Keggin heteropolyblue was originally attributed to a multiroute superexchange mechanism. Later on it was demonstrated that the large spin-triplet gap could originate from the interplay between Coulombic repulsion and electron transfer, provided the transfer routes have a certain relation in sign and magnitude.[25,26] Indeed, while the electrons are far away from each other at all times in the ground state, the possible electron transfer routes are different for singlets and triplets, and the result is a strong stabilization of the singlet.

This study of the electron pair delocalization was also performed on similar systems such as the Dawson–Wells polyanion. In this system the movement of electrons is focused on the two central 6-membered rings. The singlet ground state stabilization is obtained for the same signs for the single-transfer parameters (if double-transfer processes are negligible) as in the case of the Keggin anion, and the delocalization of the electron pair implies that an electron is delocalized over each 6-membered ring to minimize Coulomb repulsion.[27]

The effect of vibronic coupling on electron location was studied for the two electron reduced Keggin anion taking into account an adiabatic approximation.[28] The conditions of singlet and triplet stabilization discussed above are strongly affected by the vibronic interactions that tend to localize the electrons and thus effectively reduce the transfer parameters. The degrees of localization prove to be different for the spin-triplet and spin-singlet states that essentially influence the magnetic properties of the reduced Keggin anion. For a strong vibronic coupling, spin-triplet states become partial or even fully localized, and fully delocalized states can be achieved only for spin-singlets. For weak vibronic coupling in all cases a fully delocalized configuration can be found. The adiabatic approximation gives very qualitative information about localization and restricts the accuracy of calculations of the magnetic characteristics and profiles of the intervalence optical bands. Recently we have presented a powerful theoretical approach to obtain an accurate solution of the dynamic vibronic problem in large scale Jahn–Teller systems. The approach uses a symmetry adapted vibronic basis to reduce the dimension of the problem.[29] The application of this procedure to the Keggin anion is being developed and it is hoped to give an accurate description of the combined JT/pseudo JT problems for the spin-singlet and spin-triplet states in this high-nuclearity system.

Due to chemical control of electron population, polyoxovanadates represent a remarkable class of high-nuclearity MV clusters. These compounds are therefore ideal systems for studying the influence of the number of delocalized electrons in the magnetic properties. The $[V_{18}O_{48}]^{n-}$ cluster (Fig. 4) forms a family of compounds from the 18 electrons fully localized member for $n = 12$ to the mixed-valence member with 10 delocalized electrons for $n = 4$.[30] This series of polyoxovanadates presents an unexpected magnetic behavior: as the electronic population is decreased, meaning a growing distance between unpaired electrons, an increasing antiferromagnetic (AF) coupling is measured. A complete study of the influence of the exchange and transfer parameters on the low-lying spin levels has been performed. A combination of *ab initio* calculations with model *t-J* Hamiltonian was used to

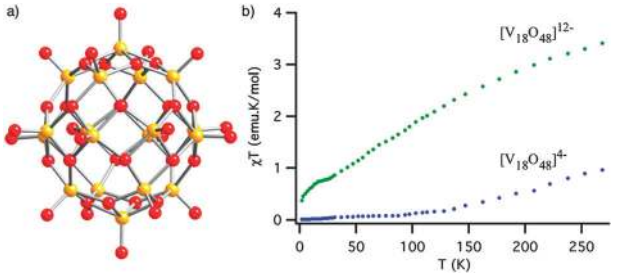

Fig. 4 (a) Structure of $[V_{18}O_{48}]^{n-}$ cluster and (b) temperature dependence of χT for the spin-localized $n = 12$ and delocalized $n = 4$ (from ref. 30).

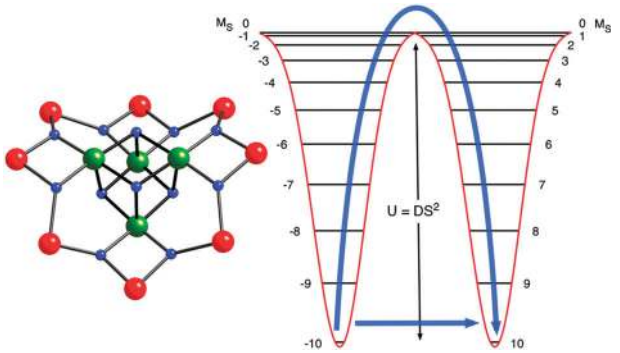

Fig. 5 Schematic structure of the Mn_{12} core and energy level scheme for the ground $S = 10$ multiplet of the Mn_{12} SMM. Two routes are possible between the wells, either the thermal route above the barrier, or a quantum tunneling shortcut.

analyze the properties of this family. The electron-transfer integral, calculated from the *ab initio* calculations, plays the key role in the macroscopic AF properties of these MV polyoxovanadates, while both the structural effect of removing electrons from the initial spin-localized cluster on the amplitude of the magnetic coupling and the effect of alleviating the spin frustration only play a minor role.[31]

In conclusion, POMs are model systems to study the interplay between electron delocalization and magnetic exchange in high-nuclearity clusters. Their highly symmetric structures facilitate the development of exact quantum-mechanical models from which a clear picture of the local parameters involved in the magnetic properties can be extracted.

2.2. Recent advances: single-molecule magnets based on POMs

Very recently the interest for these two classes of magnetic POMs has moved from their use as model systems in molecular magnetism towards the design of single-molecule magnets (SMMs) and their use as molecular spin-qubits in nanospintronic devices. In this section we will summarize the major breakthroughs achieved in the area of molecular nanomagnets, while the aspects related with the spin-qubits will be presented in a final section specifically devoted to the discussion of the relevance of POMs in spintronics and quantum computing.

The magnetic behavior of SMMs is characterized by the presence of slow-relaxation of the magnetization at low temperatures (superparamagnetic blocking) giving rise to a magnetic memory effect similar to that found in hard magnets, together with quantum tunneling effects. The most quoted example, which dates back to the early nineties, is $[Mn_{12}O_{12}(O_2CMe)_{16}(H_2O)_4]$ (Mn_{12}),[32] a molecule that combines a high axial anisotropy and a high spin ground state.[9] This molecule has been the subject of many magnetic and structural studies.[33–35] The magnetic cluster is formed by eight Mn^{3+} ions ferromagnetically coupled (external ring) and four Mn^{4+} ions in the central cube also ferromagnetically coupled. Coupling between these two moieties is antiferromagnetic, leading to a total ground spin of $S = 10$. Thus, owing to the uniaxial anisotropy of Mn_{12}, characterized by a negative D value, this S splits into its M_s components in such a way that the M_s doublet $= \pm 10$ is stabilized and becomes the ground spin state of the cluster, while the rest of spin sublevels becomes more and more excited as $|M_s|$ decreases (Fig. 5). Such a spin structure creates an energy barrier of about 50 cm^{-1} that needs to be overcome to reverse the orientation of the magnetic moment (from $M_s = +10$ to $M_s = -10$). That explains the superparamagnetic blocking observed at low temperatures in these nanomagnets and the occurrence of a magnetic hysteresis. At the same time, the presence of quantum-tunneling effects allows the spin reversal to occur without the need of overcoming the barrier.

Shortly after the magnetic characterization of Mn_{12}, an octanuclear iron complex $([Fe_8O_2(OH)_{12}(tacn)_6]^{8+}$ with tacn representing 1,4,7-triazacyclononane)[36] was also found to display SMM properties with more pronounced quantum effects.[37,38] Later, a rising number of lower nuclearity cluster systems were reported to behave as SMMs, for instance, the tetranuclear complex $[Mn_4(O_2CMe)_2(pdmH)_6](ClO_4)_2$, where $pdmH_2$ is pyridine-2,6-dimethanol.[39] The major synthetic challenge in this field was to increase the energy barrier and, consequently, the blocking temperature T_B, by designing molecules having the maximum values of S and D. In this context, many examples of magnetic clusters with larger and larger nuclearities were reported[40–43] in an attempt to increase the spin state of the cluster and hence, the superparamagnetic barrier. However, the success of this approach has been very limited as demonstrated by the fact that Mn_{12} is still among the systems exhibiting the highest effective barriers (*ca.* 45–50 cm^{-1}) and hysteresis up to 4 K. More recently magnetic clusters containing highly anisotropic lanthanoid ions have also been synthesized.[44–48] These complexes have shown effective barriers as high as 100 cm^{-1} and hysteresis up to 8 K.

In the POM area some examples of magnetic clusters exhibiting a SMM behavior have recently been described. Thus, a small number of high-spin, high-anisotropy POMs have been characterized as, for instance, the $[Mn^{III}_4Mn^{II}_2O_4(H_2O)_4]^{8+}$ cluster embedded in a POM,[49] a couple of iron(III) with hexa and nonanuclearity, $[Fe_4(H_2O)_2(FeW_9O_{34})_2]^{10-}$ and $[(Fe_4W_9O_{34}(H_2O))_2(FeW_6O_{26})]^{19-}$, respectively,[50] a cobalt(II) with hexadecanuclearity, $[\{Co_4(OH)_3PO_4\}_4(PW_9O_{34})_4]^{28-}$,[51] and a heptanuclear manganese(III)–manganese(IV) cluster, $[(\alpha\text{-}P_2W_{15}O_{56})Mn^{III}_3Mn^{IV}O_3(CH_3COO)_3]^{8-}$.[52] Although, these magnetic clusters add some new examples to the hundreds of already known SMMs, their novelty in the field of SMMs is very limited due to the very low energy barriers (10–12 cm^{-1}) they exhibit and to the lack of other interesting effects coming from the POM ligand.

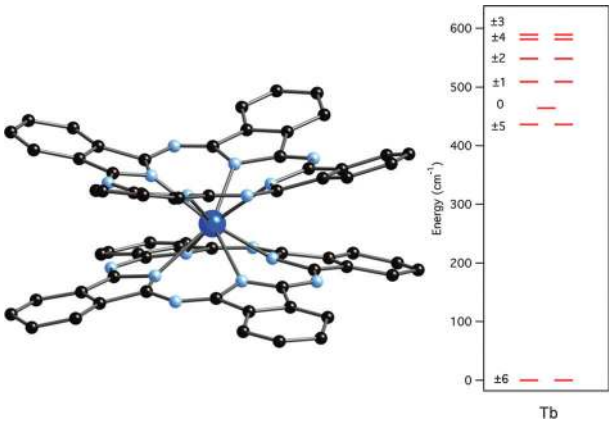

Fig. 6 Structure of terbium phthalocyaninato derivative and energy level scheme for the ground $J = 6$ multiplet.

This result contrasts with the key role that POM chemistry is playing in the new generation of SMMs known as Single-Ion Magnets (SIMs). These systems represent the limit in the miniaturization of a nanomagnet since a mononuclear complex formed by a single magnetic center, instead of a magnetic cluster, has been shown to be sufficient to behave as a SMM. The first example of this kind was reported by Ishikawa *et al.* in 2003 in the lanthanoid complexes of general formula $[LnPc_2]^-$, with a 'double-decker' structure and phthalocyanines as ligands (Fig. 6).[53] Thus, the antiprismatic D_{4d} crystal field induced by the eight coordinated atoms around the Ln^{3+} splits its ground magnetic state, characterized by the total angular momentum, J, into $\pm M_J$ sublevels. In some cases this leads to a sublevel scheme in which the levels with the higher $|M_J|$ values are stabilized with respect to the levels with the lower $|M_J|$ values. This creates a barrier that explains the SMM behavior observed in the Tb derivative for which the ground magnetic doublet corresponds to that with the maximum M_J value ($= \pm 6$), being separated from the first excited level ($M_J = \pm 5$) by more than 300 cm^{-1} (Fig. 6).

In view that POM chemistry also provides lanthanoid complexes with antiprismatic D_{4d} symmetry, we decided to study the magnetic properties of the series $[Ln(W_5O_{18})_2]^{9-}$, in short LnW_{10} (Fig. 7). Thus, in 2008 we discovered a second family of SIMs, whose best example was the Er derivative.[54] This compound exhibited a slow relaxation of the magnetization at low temperatures and a frequency-dependent out-of-phase susceptibility signal, χ'' (Fig. 8), which agrees with the presence of an energy barrier for the reversal of the magnetization ($U_{eff} = 38.5$ cm^{-1}) very close to that observed for the archetypical Mn_{12} cluster ($U_{eff} \approx 50$ cm^{-1}).[55] This key result showed that the concept of SIMs was not restricted to the bisphthalocyaninato molecules and motivated since then the search for other mononuclear complexes exhibiting SMM behavior. Nowadays, this is becoming a hot topic in molecular magnetism which has led to the discovery of tens of SIMs having different coordination geometries and different types of ligands,[56–58] thus demonstrating that the SIM concept is quite general and can also be extended to other anisotropic metal ions in axial environments, such as mononuclear uranium complexes[59,60] and mononuclear d-transition metals.[61,62]

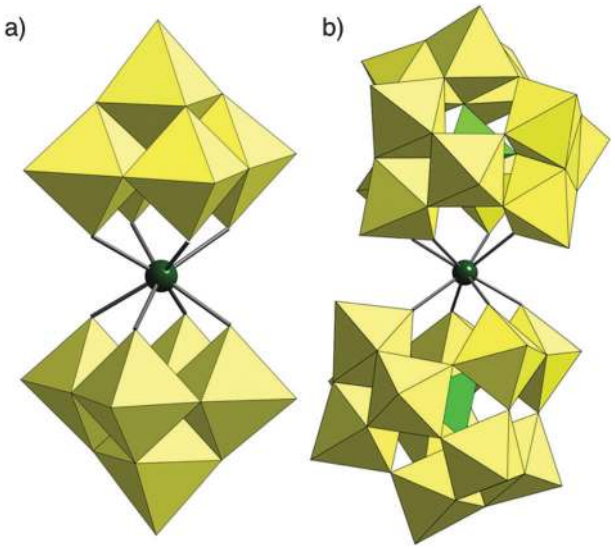

Fig. 7 Structures of $[Ln(W_5O_{18})_2]^{9-}$ and $[Ln(\beta_2\text{-}SiW_{11}O_{39})_2]^{13-}$ derivatives.

Coming back to the $[Er(W_5O_{18})_2]^{9-}$ complex, it is interesting to discuss why this system exhibits a SMM behavior, while in the $[LnPc_2]^-$ series this behavior is observed for the Tb derivative. The reason for this difference lies in the different distortion of the antiprismatic site. Thus, the antiprism formed by 8 nitrogen atoms in the bisphthalocyaninato molecules has a height $d_{pp} = 2.76$ Å, which is very similar to the square side $d_{in} = 2.80$ Å. In contrast, in the polyoxometalate $[Ln(W_5O_{18})_2]^{9-}$ the 8 oxygen atoms form a compressed antiprism, with $d_{pp} = 2.47$ Å *vs.* $d_{in} = 2.86$ Å (Fig. 9). This small structural change leads to different LF parameters and, in particular, to a change of the sign of the second order axial ZFS parameter, A_2^0 (which is related to the more familiar ZFS parameter D). As a consequence, the lowest-lying energy levels for Er and Tb are very different and almost reversed in the two classes of complexes. In fact, while in the case of Er the POM ligands stabilize larger $|M_J|$ values ($\pm 13/2$, $\pm 15/2$), the phthalocyaninato ligand stabilizes the lowest value, $M_J = \pm 1/2$. In a similar way, in the Tb case, the POM derivatives stabilize the singlet $M_J = 0$, while the doublet with the largest J value, $M_J = \pm 6$, becomes the ground state in the phthalocyaninato derivative. That explains why in the POM series, the Er behaves as a SMM, while the Tb not.

We have extended this research to the Keggin-type series $[Ln(\beta_2\text{-}SiW_{11}O_{39})_2]^{13-}$ (Ln(III) = Dy, Ho, Er, and Yb)[63] in order to study the influence of the distortion of the antiprismatic site on the spin relaxation processes. One can notice that the spin relaxation processes are faster in POMs than in the phthalocyaninato complexes showing SMM behavior. The reason may be related to the smaller separation between the lower-lying energy levels caused by the LF splitting, which in POM derivatives often contain two or more levels separated by less than 30 cm^{-1}. Another related question is the observation that, in general, for a given lanthanide, the magnetization of the Keggin-type series relaxes faster than that for the Lindqvist one. This is due to the presence of non-axial distortions in the Keggin-type derivatives (the two coordinating

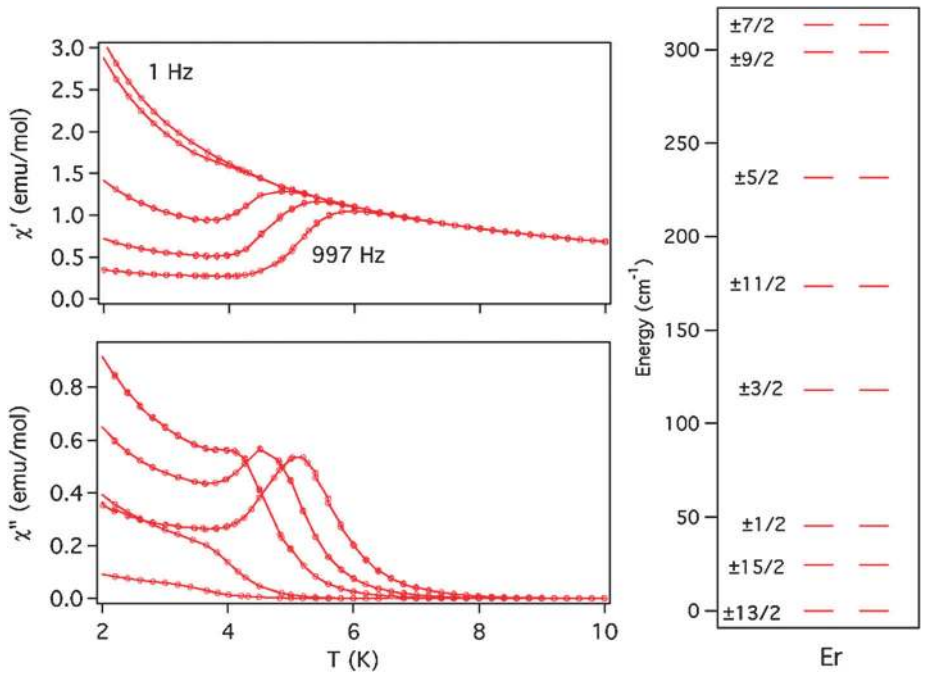

Fig. 8 In-phase and out-of-phase dynamic susceptibility of $Na_9[Er(W_5O_{18})_2]\cdot xH_2O$ at high-frequency measurements from left to right: 1, 10, 100, 332, 997 Hz and energy level scheme for the ground $J = 15/2$ multiplet.

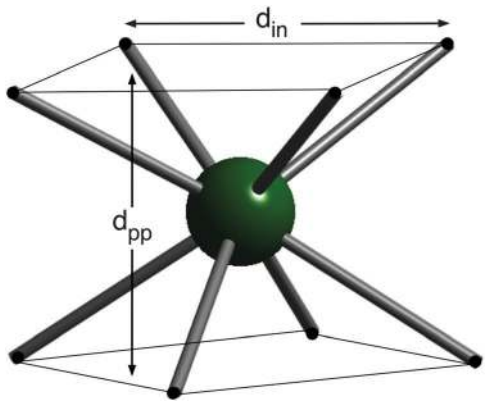

Fig. 9 Detail of the coordination structure of approximate D_{4d} symmetry, a square antiprism of side d_{in} and height d_{pp}.

planes are not parallel). In fact, apart from having a non-negligible influence on the sublevel structures, this distortion can also mix the different wave functions, therefore enhancing the quantum tunneling. Table 1 shows the most important structural parameters for some members of both series. We can see that the main difference between the two series is the larger deviation from perfect symmetry D_{4d} in the case of the Keggin series members, and also a slightly lower axial compression that results in a lower second-order crystal parameter.

Table 1 Some structural parameters concerning the lanthanide coordination sphere in the $[Ln(W_5O_{18})_2]^{9-}$ and $[Ln(SiW_{11}O_{39})_2]^{13-}$ series. Where ϕ is defined as the relative orientation between the two squares defined by the coordinating oxygen atoms and φ is defined as the angle between the normal vectors of the oxygen-based square planes

	d_{in} (Å)	d_{pp} (Å)	ϕ (°)	φ (°)	$A_2^0r^2$ (cm^{-1})
$[Dy(W_5O_{18})_2]^{9-}$	2.876	2.496	44.0	0.0	−153.6
$[Er(W_5O_{18})_2]^{9-}$	2.856	2.469	44.5	0.0	−387.2
$[Tb(SiW_{11}O_{39})_2]^{13-}$	2.833	2.458	44.6	2.8	−11.3
$[Er(SiW_{11}O_{39})_2]^{13-}$	2.832	2.478	42.5	2.8	−242.2

A final point that deserves to be discussed concerns the divergence in χ'' observed in this class of mononuclear lanthanide SMMs at temperatures below the blocking temperature. Such a behavior is specific for this class of SMMs and is in sharp contrast to that observed in the cluster-based SMMs (Mn_{12}, for example) in which χ'' tends to vanish below the blocking temperature. In the mononuclear lanthanide SMMs, both processes, the thermally activated relaxation process giving rise to the observation of a maximum in χ'', due to the superparamagnetic blocking of the magnetic moments, and a very fast quantum tunneling process within the $\pm M_J$ ground-state doublet giving rise to a divergence in χ'', seem to coexist. It is remarkable that the spin relaxation in the quantum tunneling regime can be tuned "*a la carte*" both chemically and physically. This unique feature has been shown in $Na_9Er(W_5O_{18})_2$ (ref. 55). Thus, it has been found that the quantum tunneling process can be blocked at low temperatures by diluting the magnetic sample in the yttrium analog, or by applying an external magnetic field. Furthermore, it has also been found that quantum tunneling provides a spin relaxation that is ten orders of magnitude more efficient than what is predicted by accepted theories. Speculative explanations for this fast spin-lattice energy flow have been proposed based on the collective emission of single phonons by a group of spins.

Notice that POM chemistry also offers other coordination geometries for lanthanoid ions different from the typical D_{4d} antiprism present in the $[LnPc_2]^-$ series and $[Ln(W_5O_{18})_2]^{9-}$ systems. An interesting case in this context is provided by the

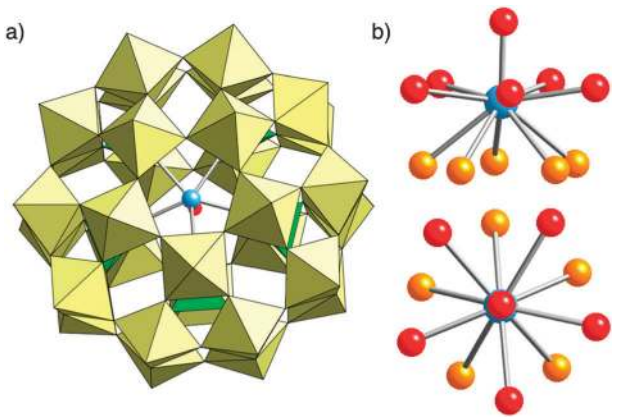

Fig. 10 (a) Structure of the Preyssler anion and (b) top and lateral views showing the near-C_{5v} coordination of the lanthanoid ion in a fivefold environment.

well-known Preyssler anion, $[LnW_{30}O_{110}]^{12-}$ (Fig. 10). This anion has a central coordination site with an unusual fivefold axial symmetry C_5. Recently we have studied both experimentally and theoretically the possibilities of preparing new SIMs based on this series.[64] In spite of the low symmetry provided by this anion, we have observed that Dy and Ho derivatives behave as SMMs exhibiting slow relaxation of the magnetization. Still, the spin dynamics, especially at low temperatures, are dominated by fast tunneling processes. To rationalize this behavior we have developed a general theoretical approach that determines the effect of the crystal field on both the splitting of the J ground state and the mixing of the resulting magnetic levels, providing at the same time an indication of the leading anisotropy parameters that control such a splitting/mixture.[65] The remarkable difference between this system and the previous one is the presence of a large off-diagonal anisotropy parameter A_6^5 due to the five fold symmetry, which mixes magnetic states with different M_J values. In addition to this off-diagonal parameter, the ground state is determined by the sign of the A_2^0 parameter. In contrast to the compounds with D_{4d} symmetry studied up to now, this family has both five oxygen ligands in equatorial positions belonging to the POM and a water molecule in an apical position. Equatorial and apical ligands contribute different signs to the A_2^0 parameter (positive for apical and negative for equatorial), giving for the case of Ho and Dy suitable conditions to stabilize the doublets with maximum M_J values.

Compared with the phthalocyaninato systems, SIMs based on POMs present several advantages: (i) The geometry around the lanthanoid is not restricted to the fourfold D_{4d} antiprism; other geometries are also possible such as the O_h cube or the fivefold axial symmetry C_5; (ii) The POM diamagnetic framework also provides a better magnetic insulation of the lanthanoid and an easy way to dilute the SIM in an isostructural matrix formed by the Y derivative; (iii) Insofar as the composition of some POM shells only includes W/Mo, O and maybe Si, they can in principle be prepared as nuclear spin-free systems. As the interaction with nuclear spins is a major source of decoherence for electron spins, these molecules are in a nearly unique position to function as model spin-1/2 systems (spin qubits) for sophisticated experiments aiming to address fundamental problems in quantum computing (this aspect will be discussed in more detail in Section 4).[66]

3. Relevance of POMs in molecular spintronics

With the recent advances in nano-fabrication of single-molecular devices, the manipulation of the spin state of a molecule has become a challenging task in molecular spintronics. An attractive way to control the spin state of a molecule is that of using electric fields or currents in order to achieve an all-electrical control of the nanodevice.[7] In fact, the use of an electric field, instead of a magnetic field, presents some advantages as it is easy to obtain (with gates or STM-tips), it undergoes fast switching ($\approx$ ps) and can be applied on the nanoscale, thus providing the possibility to address selectively a single molecule. Still, very few magnetic molecules have been proposed for this purpose, with none of these proposals having been experimentally demonstrated. These electrically responsive magnetic molecules are the following: (1) spin-crossover metal complexes,[15] (2) valence-tautomeric metal complexes,[67] (3) mixed-valence metal complexes[68–71] and (4) dipolar metal complexes, as for example asymmetric dimers[72] or molecular triangles formed by three antiferromagnetically coupled spins.[73] Notice that the most relevant examples for classes 3 and 4 are provided by POM chemistry. In fact, MV POMs may be ideal magnetic molecules to study the electrical control of the spin state. In this section we present some examples of MV POMs that can change their ground spin state by the application of an external electric field, or electric injection of extra electrons. For magnetic switching, one needs to stabilize two levels with different electronic properties that are close enough in energy to overcome this difference by applying an electric stimulus.

A first possibility is that of reducing the singlet-to-triplet gap in the two-electron reduced POMs. This can be achieved

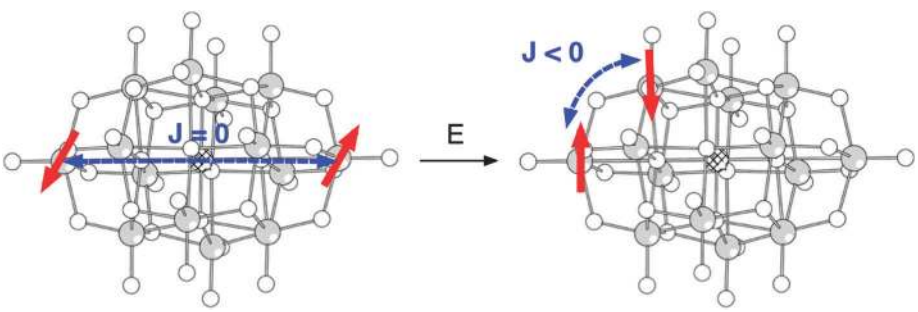

Fig. 11 Structure of the two electron reduced $[GeV_{14}O_{40}]^{8-}$ anion and electron position and interactions before and after electric field.

by separating the two electrons at farther positions in the anion, reducing thus their delocalization. An example of this kind is provided by the direduced $[GeV_{14}O_{40}]^{8-}$ (Fig. 11, right).[74] In this MV cluster the two electrons do not interact with each other; thus, the two $S = 1/2$ spins are independent and the compound is paramagnetic. This system was studied by *ab initio* calculations on embedded fragments. Surprisingly, both the connectivity of the molecule and the magnitude of most parameters in the Hamiltonian are similar to those of decatungstate, which is diamagnetic.[75] And yet the diagonalization of the *t-J* Hamiltonian for the whole molecule using the *ab initio* parameters resulted in two independent $S = 1/2$ spins, in full agreement with the experimental result. The key to explaining this apparently anomalous behavior lies in the central square $[GeV_4O_{12}]$ of the cluster, which is sandwiched between the two square pyramids $[V_5O_{14}]$. Because of a combination of poor electron transfer between the two square pyramids and a high orbital energy of the central square, the two electrons behave as independent. When an electric field is applied along the main axis of this POM, our theoretical calculations predict that the electronic distribution changes in such a way that the spins are forced to approach and to be strongly coupled. Thus, an electric field of the order of 10 V nm^{-1} is predicted to cause a sharp crossover from a paramagnetic state to an antiferromagnetic $S = 0$ state. Although in the present example the magnitude of this electric field is too strong, a way to reduce it could be by increasing the size and the asymmetry of the POM, as these effects are expected to decrease the Coulomb repulsion between the two spins when they will be forced to be antiferromagnetically coupled.

A second example is provided by $[PMo_{12}O_{40}(VO)_2]^{q-}$ (Fig. 12). In this POM, two $(VO)^{2+}$ sit at opposite tetragonal sites of the Keggin anion and host an $S = 1/2$ spin. On the other hand, the central Keggin structure $PMo_{12}O_{40}$ can act as an electron acceptor giving rise to a MV cluster able to accommodate a variable number of electrons. Thus, when the number of injected electrons is odd, the delocalized spin of the central Keggin cluster will be strongly coupled with the two localized spins located at the $(VO)^{2+}$. As a result, these two distant spins will be ferromagnetically coupled. In turn, if the number of injected electrons is even, the coupling between the localized spins will be very weak. The injection of electrons can be performed through the tunneling current provided by a STM setup. Hence, in this device a control of the exchange interaction through injection of electrons can be achieved. The use of this kind of device as an electrically addressable quantum gate will be discussed in the next section.

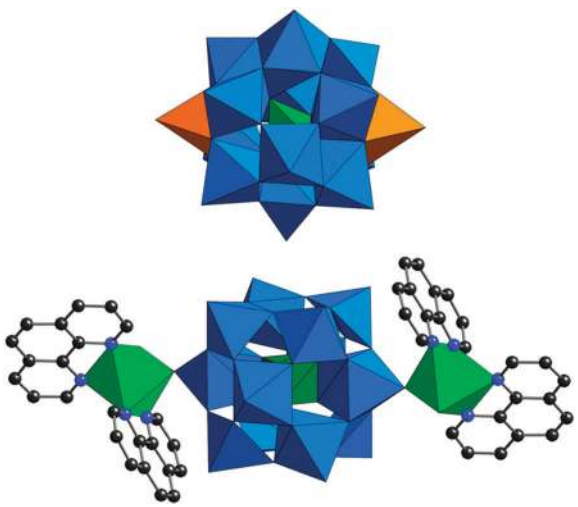

Fig. 12 Structure of $[PMo_{12}O_{40}(VO)_2]^{q-}$ and $[PMo^{VI}{}_{11}Mo^{V}O_{40}\{Ni(phen)_2(H_2O)\}_2]$ anions.

Finally, a third example of a switchable magnetic POM is provided by the new bicapped mixed-valence polyoxometalate $[PMo^{VI}{}_{11}Mo^{V}O_{40}\{Ni(phen)_2(H_2O)\}_2]$ where two Ni^{2+} ($S = 1$) are placed in two opposite MoO_6 positions. In this case, a compound with an odd number of delocalized electrons has been isolated, and, as expected, the "extra" electron, which is fully delocalized at room temperature, is simultaneously coupled antiferromagnetically with the two $S = 1$ sites. The result is an effective $S = 3/2$ ground state (two parallel spins $S = 1$ antiferromagnetically coupled to a central spin $S = 1/2$). At temperatures around 10 K, a trapping of this central spin near one Ni^{2+} center occurs as a consequence of the vibronic coupling. As a consequence, the magnetic communication between the Ni^{2+} centers is effectively switched off so the ground state corresponds to that of two independent spins: an $S = 1/2$, coming from the antiferromagnetic coupling between the $S = 1$ and the trapped spin $S = 1/2$, and an $S = 1$ from the second Ni^{2+} center. In this case the switch between the different spin states is thermally controlled.

4. Relevance of POMs in quantum computing

4.1. Molecular spin qubits

Quantum computing consists of the explicit use of quantum mechanical phenomena – such as quantum superposition and entanglement – for the purposes of information technology.[76] The coherent manipulation of quantum systems would enable quantum information processing, which for a series of problems notably including the simulation of quantum systems themselves is qualitatively more efficient than classical information processing. The basic pieces of quantum computing are *quantum bits and quantum gates*, analogous to classical bits and logic gates. A quantum bit or qubit is a two-level system, *e.g.* a spin $S = 1/2$; a quantum gate is a logic operation between two or more such qubits. A typical example is the Controlled-NOT gate, where the target qubit is flipped from $|0\rangle$ to $|1\rangle$ and *vice versa* if and only if the value of the control qubit is $|1\rangle$ (Fig. 13).

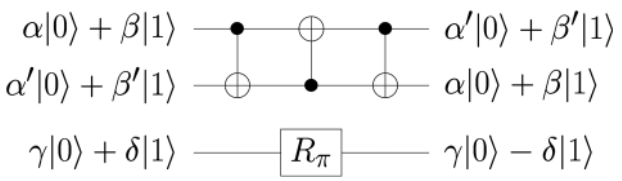

Fig. 13 Sample fragment of a quantum circuit illustrating the effect of some typical quantum gates: a "SWAP" operation between the upper and center qubits is effected through three consecutive "controlled-NOT" operations, while the lower qubit suffers a simple phase rotation. Dark dots mark control qubits, empty circles mark target qubits.

Two extremely challenging requisites needed for useful qubits are a long quantum coherence time and the possibility to scale up the system to many hundreds of qubits that can be manipulated in a non-trivial way. *Scalability* is mostly an engineering problem, which from the point of view of chemistry translates simply into extremely sophisticated processability. Here, we shall focus on *decoherence* instead. Decoherence can be defined as the loss of the fragile quantum phase information because of an uncontrolled entanglement with its environment. It is a fundamental physical problem, with deep philosophical consequences.[77] We still lack a general analysis of every relevant mechanism of decoherence, but much progress is being made in some areas such as that represented by the SMMs.[78] The most used experimental parameter to estimate the decoherence time is the spin–spin relaxation time T_2, which in combination with the oscillation frequency permits to estimate the average number of oscillations before the system loses quantum phase information.

Over the past few decades, physics has offered a large range of quantum bits such as trapped ions or trapped atoms, quantum dots, quantum optical cavities, rf SQUIDs and, notably, nitrogen-vacancy defects on diamond. To learn more about physical qubits, the reader is referred to excellent reviews such as ref. 79 and references therein. Over the same timeframe, chemistry has proposed, synthesized and studied a wide variety of proof-of-principle systems in the field of molecular spin qubits and quantum gates. In this context, the chemical bottom-up approach consists of studying and understanding individual spin qubits first, building up toy models with one or a few quantum gates next, and finally working towards organization to aim for scalability.

In the rest of this review we will focus on electron spin qubits, but, given its relevance in chemistry, one needs to briefly mention NMR quantum computing since it was precisely here where molecules played a key role in the early successes of Quantum Information Processing.[80] The reason behind these results is the recontextualization of technical expertise. NMR scientists already had decades of experience with powerful pulse sequences that use phenomena such as population inversion, quantum transfer or spin–lattice relaxation. Often, these sophisticated sequences, designed to extract information about complicated molecules, could be used for coherent manipulation of the quantum states of the molecular nuclear spins.

Before reviewing the existing examples of molecular spin qubits, a very brief explanation of the mechanisms of decoherence for these systems is necessary; for more details the reader is referred to ref. 66. Broadly speaking, the three decoherence sources for these systems are spin bath decoherence, oscillator bath decoherence and pairwise dipolar decoherence. They can be regulated by a combination of temperature, magnetic field and chemical design of the system.[78] The spin bath mainly consists of nuclear spins, but, in general, it also includes any localized excitation able to couple to the qubit state, *e.g.* a crystallographic disorder, or the spin of a paramagnetic impurity. It causes precessional decoherence, topological decoherence and noise decoherence. Precessional decoherence, the most important of the three, is non-dissipative and is described as the spin bath absorbing phase information from the qubit. Note that only noise decoherence is directly related to the well-known T_1/T_2 characterization. In insulators, the oscillator bath is mainly the phonon bath. For conductors, the temperature-independent Ohmic bath typically contributes very strongly to decoherence, so it is usually safer to avoid conductors. Pairwise dipolar decoherence is caused by distant qubits being resonant and thus having a probability of spin-flip. This phenomenon is not solved by mere dilution and requires either low dimensionalities, or sophisticated quantum error correction procedures, or both.

In the context of quantum computing, molecular nanomagnets offer various potential advantages over other spin systems. These are strongly coupled spin clusters that function at low temperature as an effective $S = 1/2$, *i.e.* single qubits. Strategies for the implementation of quantum algorithms in such nanoscale magnets have been described by A. Ardavan *et al.*[81] The determination of the phase relaxation time appropriate for an individual molecular spin is essential. Experiments utilizing pulsed ESR techniques show that the phase relaxation times in at least some molecular magnets are long enough to permit multiple qubit operations to be performed; these operations would also take place *via* EPR pulses. Coherent manipulation of the spin in SMMs by using Landau–Zener transitions, which provides the possibility to tune the resulting magnetization due to quantum interference effects, has also been theoretically discussed.[82]

Interesting examples about the deployment of molecular nanomagnets in quantum information have been performed in Cr_7M heterometallic wheels (see Fig. 14), with M = Ni or Mn, where phase-coherence relaxation is dominated by the coupling of the d electron spin to protons within the molecule.[83] In these systems, at low temperatures and for perdeuterated samples, excellent $T_2 = 3.8$ μs were measured.

A related $S = 1/2$ system is the antiferromagnetic V_{15} POM, where decoherence times are in the order of $T_2 = 0.1$ μs. This system will be presented in more detail later on.

Another example is provided by the SMM Fe_8. In this nanomagnet coherence times of the order of $T_2 = 0.5$ μs at $T = 1.2$ K and transverse fields of the order of $H = 10$ T. Through a theoretical and experimental study, it was found that at this magnetic field, phonons are the main source of

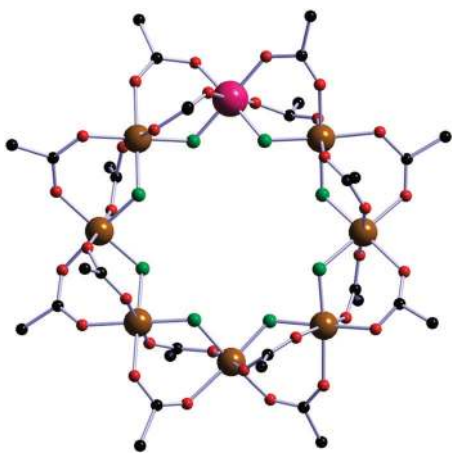

Fig. 14 Structure of the Cr_7M heterometallic wheel.

decoherence at temperatures below 1.2 K and magnons – intermolecular dipolar interactions – dominate at higher temperatures. The theoretical treatment allows the exploration of the parameter space for further optimization. With an adequate transverse field and at $T < 0.13$ K, times up to $T_2 = 50$ μs would be expected. In these conditions, the nuclear spins are the main source of decoherence, so that perdeuteration would extend coherence even further, to $T_2 = 500$ μs.

Due to the fast development of the field, several chemical quantum computation reviews using magnetic molecules as spin qubits have been published over the past decade, covering both experimental and theoretical results.[66,81,84]

As far as the quantum gates are concerned, research on multi-qubit molecules starts with the synthesis and characterization of systems which seem to embody more than one qubit, *e.g.* systems with weakly coupled electron spins. The next step is usually the preparation of actual entanglement *i.e.* of non-trivial superpositions that involve more than one qubit. A preliminary but complete task would be the implementation of a full process of initialization, quantum gating and readout. To build a useful quantum computer one would need to scale up the system indefinitely, so a criterion to evaluate partial achievements is whether one can build upon them to get closer to that ultimate goal.

An influential theoretical work by Leuenberger and Loss proposed the implementation of a (multi-qubit) Grover database search algorithm using pulsed ESR on the low-energy $S = 10$ manifold of just one Mn_{12} (or Fe_8) single molecule magnet.[85] Using an *ad hoc* coding scheme, one would encode up to $2^{2S-2} > 10^5$ numbers in $2S+1 = 21$ sublevels with a complicated pulse sequence. A single EPR pulse would be able to decode the information, so that the Grover database search algorithm would be used as a data compression tool. More recently, other ideas in the field of quantum information processing have developed on spin–electric effects for the electrical control of either molecular nanomagnets[86] or molecular antiferromagnets.[87]

Several studies have been developed concerning SIMs. There exist full quantum computing proposals, including interactions between spin qubits in the solid state, which would also be applicable to a molecular crystal based on lanthanoid SIMs.[88]

On a smaller scale, the capability to implement a Controlled-NOT quantum logic gate using molecular clusters containing two Tb^{3+} ions was demonstrated (see Fig. 15).

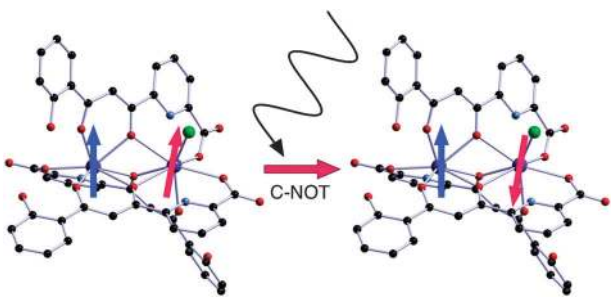

Fig. 15 An EPR pulse can reverse the orientation of the magnetic moment of a Tb^{3+} ion, provided its neighbour is pointing "up", this selective switching being equivalent to the quantum logic gate Controlled-NOT (C-NOT).

Here the definition of control and target qubits is based on the strong magnetic anisotropy and the magnetic inequivalence of both ions, which also provides a method to realize a SWAP gate in the same cluster.[89] An introduction to the requirements for a paramagnetic molecule to act as a 2-qubit quantum gate is proposed in a tutorial review published by G. Aromí *et al.*, where two synthetic strategies are presented, based on ligand design and inorganic synthesis, preparing dinuclear complexes of anisotropic metal ions that present dissimilar environments and magnetic coupling.[90]

4.2. Polyoxometalates as spin qubits

A distinctive advantage of POMs is the possibility of combining a rich magnetochemistry with an environment that is relatively free of nuclear spins. Indeed, nuclear spins are one of the main sources of decoherence for molecular spin qubits and it is not trivial to get rid of them, as every isotope of every element with an odd number of protons bears a nuclear spin.[66] In POMs this can be achieved by avoiding heteroelements like phosphorus, and instead relying on Mo and W POMs where the natural abundance of their $I = 0$ isotopes are high. Moreover, in the salts crystallization water molecules and alkali counterions should also be minimized. Of course, crystalline solids, such as simple or ternary oxides, can also be free of nuclear spins, but these typically lack the flexibility of molecular chemistry.

It is not uncommon that the same molecule can be seen either as a nanomagnet or as a spin qubit. Here we will discuss the possibility of using the two types of magnetic POMs presented in Section 2 as possible spin qubits. In the spin-localized POMs, the manipulation can take place through time-dependent magnetic fields, *i.e.*, EPR pulses. These are analogous to other molecular spin qubits presented earlier. In the spin-delocalized MV POMs, the extra electrons enable a manipulation through a time-dependent electric field, which allows a more detailed temporal and geometrical control.

Focusing on spin-localized POMs, recent observations have demonstrated the possibility of using as qubits POM cage

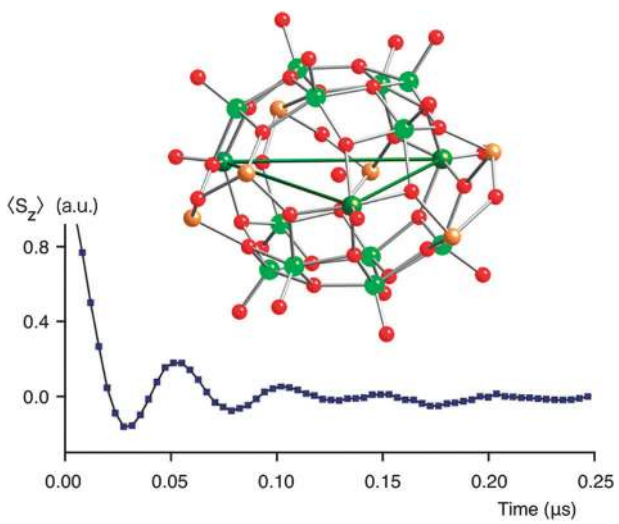

Fig. 16 Structure of V_{15} POM spin qubit candidate and time evolution of the average spin $\langle S_z \rangle$ after a spin–echo sequence (from ref. 92).

complexes with an $S = 1/2$ ground state. One example is provided by the $\{V_{15}\}$ SMM (Fig. 16).[91] Each cluster contains 15 antiferromagnetically coupled $S = 1/2$ spins, leading to an $S = 1/2$ collective ground state. When this system is placed into a resonant cavity, the microwave field induces oscillatory transitions between the ground and excited collective spin states (Rabi oscillations), indicative of long-lived quantum coherence (Fig. 16).[92] The theoretical analysis allowed a rough estimation of the different contributions to decoherence of the ^{1}H and ^{51}V nuclear spins, which in this case dominates over the phonons and dipolar interactions. Later, a model of spin–vibronic relaxation was proposed which allowed a detailed study of the mechanism of phonon-mediated relaxation in this system.[93] Recently, it has been possible to distinguish between the Rabi oscillations of the ground state $S = 1/2$ ($T_2 = 149$ ns) and the first excited state $S = 3/2$ ($T_2 = 187.7$ ns) in a frozen trichloromethane solution at 2.4 K.[94]

Simpler molecular nanomagnets are provided by the mononuclear lanthanoid complexes described in Section 2. In these POMs the control over the spin–lattice relaxation in the quantum regime, studied in ErW_{10}, indicated that these SIMs are promising candidates to act as the hardware for quantum information.[55] In fact, Rabi oscillations were observed in the Ho derivative indicating long decoherence times as a consequence of the large tunneling splitting of the ground state of this SIM (*ca.* 0.3 cm^{-1}).[95]

In addition, the family of Preyssler POMs of general formula $[Ln(P_5W_{30}O_{110})]^{12-}$ (in short: LnW_{30}) shows, as pointed out above, an unusual fivefold molecular symmetry (see Fig. 10), which gives rise to remarkably large off-diagonal anisotropy parameters of the fifth order. In the case of TbW_{30}, the ground-state doublet is found to be $M_J = \pm 5$. This means that a strong mixing occurs in the ground doublet, with the participation of $M_J = 0$. As a consequence, the tunneling splitting of this ground state is extraordinarily large ($\Delta \approx 2$ cm^{-1}), orders of magnitude larger than that typically found for cluster-type SMMs (of the order of 10^{-4} to 10^{-6} cm^{-1}).[64] The spin dynamics, especially at low temperatures, is then dominated by fast tunneling processes. This feature is detrimental for their use as (classical) magnetic bits. However, it can provide very attractive candidates for the application as solid-state spin qubits. In fact, the high tunneling rates should enable the coherent manipulation of these two states, by for example using external electromagnetic radiation. Note that two of the main mechanisms for decoherence, namely interaction with nuclear spins and with neighboring spin qubits, are strongly quenched by this large tunneling splitting.[80]

Also of interest, for different reasons, are the cases of GdW_{30} and GdW_{10}. In these systems the magnetic anisotropy arises *via* the quantum mixture of the ground state with excited multiplets having a nonzero orbital momentum, a process that is usually neglected in lanthanoid SIMs. For GdW_{30}, this results in an easy-plane anisotropy, while GdW_{10} displays an easy axis magnetic anisotropy.[96] Both compounds show the typical SMM behavior at low temperatures (with a frequency-dependent χ'' signal). Of course, as this effect arises from a mixture with excited states, the anisotropy is rather weak and can only be observed at sub-Kelvin temperatures. In the case of GdW_{30}, even at 200 mK the relaxation rate is still temperature-dependent. These systems were also analyzed as qubit candidates, and decoherence times of the order of $T_2 = 410$ ns were found for diluted samples, at 6 K and with an applied field of 0.1 T. A figure of merit $Q_M = 2\Omega_R T_2 > 50$ was determined, where W_R is the frequency of coherent oscillation for a radiofrequency field $h_{rf} = 1$ mT and T_2 is the spin–spin relaxation time. This parameter is related to the number of coherent quantum operations we are able to perform.[96]

4.3. Qu-gates on polyoxometalates

In the previous discussion we have shown that magnetic POMs can provide useful examples of spin qubits. Here we will take advantage of the possibility of POMs to obtain several spins that can act as qubits to develop some quantum operations by coupling these spins. The starting point for this purpose will be to use those POMs in which an electric control of this spin coupling can be achieved (see Section 3).

A first example is provided by $[PMo_{12}O_{40}(VO)_2]^{q-}$ connected to an electric circuit through a STM set up (Fig. 17). As we have pointed out above, in this device one can control the magnetic coupling between the two spins located at the $(VO)^{2+}$ sites through an electric tunneling current that injects a controlled number of electrons in the central MV Keggin cluster.[70]

Adding an accurate time control to this spintronic switch, it can be used as a quantum gate. At the starting point of the graph in Fig. 17 the Keggin cluster has an even number of electrons; this can be achieved with the help of a backgate potential. The quantum operation begins by changing the gate

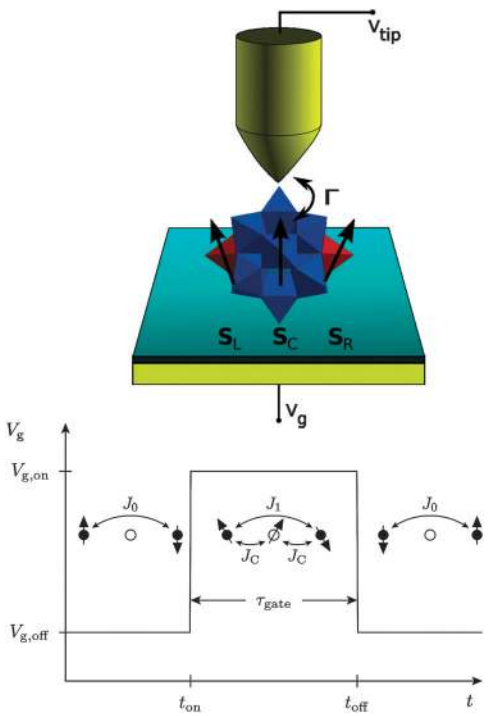

Fig. 17 Top: proposed setup to effect two-qubit gates onto $[PMo_{12}O_{40}(VO)_2]^{q-}$, a mixed-valence POM that combines two localized electrons on the lateral vanadyl groups with a variable number of delocalized electrons in the Keggin core. Bottom: during τ_{gate} the voltage is $V_{g,on}$ and the Keggin structure hosts an extra electron, which induces a rapid exchange of the vanadyl spins.

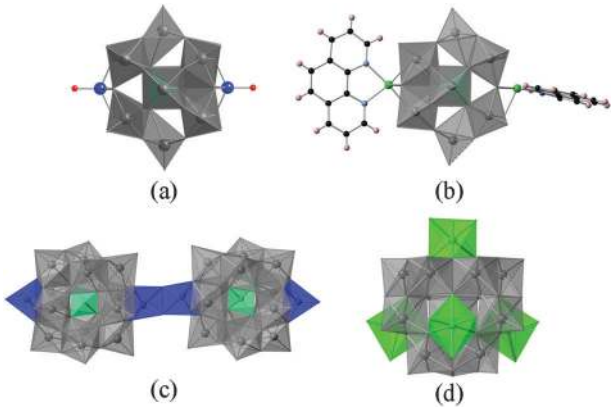

Fig. 18 POMs where two or more localized magnetic moments are linked by polyoxomolybdate units capable of hosting one or more delocalized electrons. (a) $[PMo_{12}O_{40}(VO)_2]^{q-}$, (b) $[PMo_{12}O_{40}(Ni(phen))_2]^{2-}$, (c) $[Si_2Mo_{24}O_{80}(VO)_4]^{8-}$, and (d) $[Mo_{12}O_{30}(\mu_2\text{-}OH)_{10}H_2(Ni(H_2O)_3)_4]$.

voltage so that an electron tunnels from the tip into the molecule, and ends at a certain τ_{gate} by reverting to the initial voltage so that the electron tunnels back out. The time needed to achieve a SWAP between the left and right spin qubits, as well as the quantum fidelity of the said operation, is a function of J_1, J_C and the tunnel coupling to the tip Γ.

Several analogue structures have been described (Fig. 18) that could serve as extensions of this scheme.[71] In these molecules the complexity of the qubit network is augmented either by using Ni^{II} ($S = 1$) instead of V^{IV} ($S = 1/2$) or by having four magnetic sites instead of two, or both. Of course, if the proposed experiments with $Mo_{12}V_2$ are already very demanding, further complications can only increase the difficulty.

One of the mentioned natural extensions is that of substituting the two $S = \frac{1}{2}$ $(VO)^{2+}$ sites by two $S = 1$ Ni^{2+} sites. The magnetic properties of the resulting cluster $[PMo_{12}O_{40}(Ni(phen))_2]^{2-}$ have been discussed in Section 3. If one operates only within the ground $M_S = \pm 1$ doublet, the Ni system seems to be very close to the V analogue. Nevertheless, the spin dynamics and even the allowed quantum processes are expected to be different between an $M_S = \pm 1/2$ and an $M_S = \pm 1$ doublet. Moreover, this system may benefit from the additional $M_S = 0$ singlet, which should enrich the quantum system.

Another example is provided by the MV POM $[GeV_{14}O_{40}]^{8-}$, which was also discussed in Section 3. In this case, just like for $[PMo_{12}O_{40}(VO)_2]^{q-}$ or $[PMo_{12}O_{40}(Ni(phen))_2]^{2-}$, the gating would also happen by the accurate control of the magnetic exchange between the two spin qubits through the application of a short-lived electric field. In quantum information terms, a SWAP gate – or its square root – could thus be performed.

5. Concluding remarks

The progress of our theoretical understanding, together with the availability of some experimental techniques, has allowed us to change our perspective on POMs and move the focus from the macroscopic to the nanoscopic scale. Indeed, while POMs have always been nano-objects, we have seen how in the history of molecular magnetism they were used merely as models for solid-state phenomena. Spin-localized POMs were studied to deepen our understanding of basic interactions such as (anisotropic) superexchange. In particular, magneto-structural analogies in series of compounds were used in combination with sophisticated Inelastic Neutron Scattering data, which proved to be sensitive not only to the magnitude and anisotropy of the exchange parameters but also to the relative orientation of the exchange anisotropy axes. Complementary processes such as electron transfer and vibronic coupling were studied in spin-delocalized POMs in the search for an understanding of the interplay between magnetic exchange and electron transfer in mesoscopic objects. For example, the magnetic properties of an extremely complex polyoxovanadate system formed by 10 spins delocalized over 18 metal sites were analyzed by means of a combined strategy of *ab initio* quantum chemistry calculations and exact diagonalizations of a model *t-J* Hamiltonian.

More recently, the impact of POMs has been evolving towards their potential applications in spintronics and quantum computing. The use of POMs as switches or spintronic components can be based on different effects:

(i) Control of the number of electrons in the system, or the oxidation state in terms more familiar to chemists, by means of a gate voltage. The best known scheme, based on $[PMo_{12}O_{40}(VO)_2]^{q-}$, defined a class of molecular systems: those where two localized spins are coupled to a redox-active unit. The scheme was exemplified using this mixed-valence POM, for which the model parameters were calculated using an *ab initio* approach; but the general principles behind this proposal also apply to non-POM molecular systems.

(ii) Control of the distribution of charge in the system by means of an electric field, which could be seen as producing a position-dependent chemical potential. In either case, an electrical contact of the molecule with an electronic circuit may provide an external control of its magnetic properties. This observation will open a new trend in unimolecular spintronics. In the future we will see more and more studies devoted to the control of the spin state of a molecule by means of an external stimulus different from a magnetic field.

(iii) Minimization of the quantum decoherence. The main problem to design qubits is the minimization of decoherence, particularly from nuclear spins and dipolar interactions. The use of molecular spin qubits offers important advantages, namely reduced decoherence and high reproducibility. Currently, research is oriented towards a better understanding of these basic yet extremely fragile building blocks. In this context, POM chemistry strives to design and offer qubits with the longest possible coherence time. In POM molecules the main sources of quantum decoherence (hyperfine couplings and dipolar spin–spin interactions) can be minimized by preparing nuclear-spin-free compounds and by diluting the magnetic centers, while conserving the crystallinity. The ability of POMs to accommodate the lanthanoids in very different symmetries (D_{4d} *vs.* C_5) also offers the possibility of tuning the magnetic anisotropy in these nanomagnets, while keeping them magnetically isolated (the magnetic ordering in these materials only occurs at very low temperatures; typically below 0.01 K).

(iv) Fabrication of quantum gates. The implementation of quantum gates can be seen as an extension of the switching devices.

Instead of aiming for a classical switching between two states (ON and OFF), a coherent quantum manipulation may happen during a controlled, short-lived OFF–ON–OFF process, thanks to the long coherence times exhibited by POM qubits.

In summary, while magnetic polyoxometalates pose complex theoretical problems and tough experimental challenges in molecular magnetism, these nanomagnets open a window for the manipulation of quantum spins at the molecular level, a nanotechnological feat that would be crucial not only in nanomagnetism but also for molecular spintronics and its applications in quantum computing.

Acknowledgements

We wish to thank our colleagues, co-workers and collaborators for the important contributions to the work reported herein. The present work has been partly funded through the Spanish MINECO (grants MAT2011-22785, MAT2007-61584, and the CONSOLIDER project on Molecular Nanoscience), the EU (Project ELFOS and ERC Advanced Grant SPINMOL) and the Generalidad Valenciana (Prometeo and ISIC Programmes).

References

1 J. Åkerman, *Science*, 2005, **308**, 508.
2 L. Prejbeanu, M. Kerekes, R. C. Sousa, H. Sibuet, O. Redon, B. Dieny and J. P. Nozières, *J. Phys.: Condens. Matter*, 2007, **19**, 165218.
3 B. Georges, J. Grollier, M. Darques, V. Cros, C. Deranlot, B. Marcilhac, G. Faini and A. Fert, *Phys. Rev. Lett.*, 2008, **101**, 017201.
4 J. R. Petta, A. C. Johnson, J. M. Taylor, E. A. Laird, A. Yacoby, M. D. Lukin, C. M. Marcus, M. P. Hanson and A. C. Gossard, *Science*, 2005, **309**, 2180.
5 C. A. Chappert, A. Fert and F. N. Van Dau, *Nat. Mater.*, 2007, **6**, 813.
6 D. D. Awshalom and M. M. Flatté, *Nat. Phys.*, 2007, **3**, 153.
7 S. Sanvito, *Chem. Soc. Rev.*, 2011, **40**, 3336.
8 J. Camarero and E. Coronado, *J. Mater. Chem.*, 2009, **19**, 1678.
9 D. Gatteschi and R. Sessoli, *Angew. Chem., Int. Ed.*, 2003, **42**, 268.
10 L. Bogani and W. Wernsdorfer, *Nat. Mater.*, 2008, **7**, 179.
11 S. Sanvito and A. R. Rocha, *J. Comput. Theor. Nanosci.*, 2006, **3**, 264.
12 S. Pramanik, C. G. Stefanita, S. Patibandla, S. Bandyopadhyay, K. Garre, N. Harth and M. Cahay, *Nat. Nanotechnol.*, 2007, **2**, 216.
13 S. Sanvito, *Nat. Mater.*, 2007, **6**, 803.
14 A. R. Rocha, V. M. Garcia-Suarez, S. W. Bailey, C. J. Lambert, J. Ferrer and S. Sanvito, *Nat. Mater.*, 2005, **4**, 335.
15 F. Prins, M. Monrabal-Capilla, E. A. Osorio, E. Coronado and H. S. J. van der Zant, *Adv. Mater.*, 2011, **23**, 1545.
16 E. Coronado and C. J. Gómez-García, *Comments Inorg. Chem.*, 1995, **17**, 255.
17 E. Coronado and C. J. Gómez-García, *Chem. Rev.*, 1998, **98**, 273.
18 J. M. Clemente-Juan and E. Coronado, *Coord. Chem. Rev.*, 1999, **193–195**, 361.
19 D. L. Long, E. Burkholder and L. Cronin, *Chem. Soc. Rev.*, 2007, **36**, 105.
20 A. Palii, B. Tsukerblat, S. Klokishner, K. R. Dunbar, J. M. Clemente-Juan and E. Coronado, *Chem. Soc. Rev.*, 2011, **40**, 3130.
21 C. J. Gómez-García, E. Coronado, J. J. Borrás-Almenar, M. Aebersold, H. U. Güdel and H. Mutka, *Phys. B*, 1992, **180**, 238.
22 H. Andres, J. M. Clemente-Juan, M. Aebersold, H. U. Güdel, E. Coronado, H. Büttner, G. Kearly, J. Melero and R. Burriel, *J. Am. Chem. Soc.*, 1999, **121**, 10028.
23 J. M. Clemente-Juan, E. Coronado, A. Gaita-Ariño, C. Gimenez-Saiz, H. U. Gudel, A. Sieber, R. Bircher and H. Mutka, *Inorg. Chem.*, 2005, **44**, 3389.
24 J. M. Clemente-Juan, E. Coronado, A. Gaita-Ariño, C. Gimenez-Saiz, G. Chaboussant, H. U. Güdel, R. Burriel and H. Mutka, *Chem. Eur. J.*, 2002, **8**, 5701.
25 J. J. Borrás-Almenar, J. M. Clemente, E. Coronado and B. S. Tsukerblat, *Chem. Phys.*, 1995, **195**, 1.
26 N. Suaud, A. Gaita-Ariño, J. M. Clemente-Juan and E. Coronado, *Chem.–Eur. J.*, 2004, **10**, 4041.
27 J. J. Borrás-Almenar, J. M. Clemente, E. Coronado and B. S. Tsukerblat, *Chem. Phys.*, 1995, **195**, 16.
28 J. J. Borrás-Almenar, J. M. Clemente, E. Coronado and B. S. Tsukerblat, *Chem. Phys.*, 1995, **195**, 29.
29 B. Tsukerblat, A. Palii, J. M. Clemente-Juan, A. Gaita-Ariño and E. Coronado, *Int. J. Quantum Chem.*, 2012, **112**, 2957.
30 A. Müller, R. Sessoli, E. Krickemeyer, H. Bögge, J. Meyer, D. Gatteschi, L. Pardi, J. Westphal, K. Hovemeier, R. Rohlfing, J. Döring, F. Hellweg, C. Beugholt and M. Schmidtmann, *Inorg. Chem.*, 1997, **36**, 5239.
31 C. J. Calzado, J. M. Clemente-Juan, E. Coronado, A. Gaita-Ariño and N. Suaud, *Inorg. Chem.*, 2008, **47**, 5889.
32 R. Sessoli, H. L. Tsai, A. R. Schake, S. Wang, J. B. Vincent, K. Folting, D. Gatteschi, G. Christou and D. N. Hendrickson, *J. Am. Chem. Soc.*, 1993, **115**, 1804.
33 J. Friedman, M. Sarachik, J. Tejada and R. Ziolo, *Phys. Rev. Lett.*, 1996, **76**, 3830.
34 L. Thomas, F. Lionti, R. Ballou, D. Gatteschi, R. Sessoli and B. Barbara, *Nature*, 1996, **383**, 145.
35 W. Wernsdorfer, T. Ohm, C. Sangregorio, R. Sessoli, D. Mailly and C. Paulsen, *Phys. Rev. Lett.*, 1999, **82**, 3903.
36 A. L. Barra, P. Debrunner, D. Gatteschi, C. E. Schulz and R. Sessoli, *Europhys. Lett.*, 1996, **35**, 133.
37 W. Wernsdorfer, A. Caneschi, R. Sessoli, D. Gatteschi, A. Cornia, V. Villar and C. Paulsen, *Phys. Rev. Lett.*, 2000, **84**, 2965.
38 W. Wernsdorfer, A. Caneschi, R. Sessoli, D. Gatteschi and A. Cornia, *Europhys. Lett.*, 2000, **50**, 552.
39 J. Yoo, E. K. Brechin, A. Yamaguchi, M. Nakano, J. C. Huffman, A. L. Maniero, L. C. Brunel, K. Awaga, H. Ishimoto, G. Christou and D. N. Hendrickson, *Inorg. Chem.*, 2000, **39**, 3615.
40 S. M. J. Aubin, M. W. Wemple, D. M. Adams, H.-L. Tsai, G. Christou and D. N. Hendrickson, *J. Am. Chem. Soc.*, 1996, **118**, 7746.
41 P. King, W. Wernsdorfer, K. A. Abboud and G. Christou, *Inorg. Chem.*, 2004, **43**, 7315.
42 A. Tasiopoulos, A. Vinslava, W. Wernsdorfer, K. A. Abboud and G. Christou, *Angew. Chem., Int. Ed.*, 2004, **43**, 2117.
43 M. Murugesu, S. Takahashi, A. Wilson, K. A. Abboud, W. Wernsdorfer, S. Hill and G. Christou, *Inorg. Chem.*, 2008, **47**, 9459.
44 P. H. Lin, T. J. Burchell, L. Ungur, L. F. Chibotaru, W. Wernsdorfer and M. Murugesu, *Angew. Chem., Int. Ed.*, 2009, **48**, 9489.
45 Y. N. Guo, G. F. Xu, P. Gamez, L. Zhao, S. Y. Lin, R. Deng, J. Tang and H. J. Zhang, *J. Am. Chem. Soc.*, 2010, **132**, 8538.
46 J. D. Rinehart, M. Fang, W. J. Evans and J. R. Long, *Nat. Chem.*, 2011, **3**, 538.
47 I. J. Hewitt, J. Tang, N. T. Madhu, C. E. Anson, Y. Lan, J. Luzon, M. Etienne, R. Sessoli and A. K. Powell, *Angew. Chem., Int. Ed.*, 2010, **49**, 6352.
48 R. Sessoli and A. K. Powell, *Coord. Chem. Rev.*, 2009, **253**, 2328.
49 C. Ritchie, A. Ferguson, H. Nojiri, H. N. Miras, Y. F. Song, D. L. Long, E. Burkholder, M. Murrie, P. Kögerler, E. K. Brechin and L. Cronin, *Angew. Chem. Int. Ed.*, 2008, **47**, 5609.
50 J.-D. Compain, P. Mialane, A. Dolbecq, I. M. Mbomekallé, J. Marrot, F. Sécheresse, E. Rivire, G. Rogez and W. Wernsdorfer, *Angew. Chem.*, 2009, **121**, 3123.
51 M. Ibrahim, Y. Lan, B. S. Bassil, Y. Xiang, A. Suchopar, A. K. Powell and U. Kortz, *Angew. Chem., Int. Ed.*, 2011, **50**, 4708.
52 X. Fang, P. Kögerler, M. Speldrich, H. Schilderb and M. Lubana, *Chem. Commun.*, 2012, **48**, 1218.
53 N. Ishikawa, M. Sugita, T. Ishikawa, S. Y. Koshihara and Y. Kaizu, *J. Am. Chem. Soc.*, 2003, **125**, 8694.
54 M. A. AlDamen, J. M. Clemente-Juan, E. Coronado, C. Martí-Gastaldo and A. Gaita-Ariño, *J. Am. Chem. Soc.*, 2008, **130**, 8874.

55 F. Luis, M. Martínez-Pérez, O. Montero, E. Coronado, S. Cardona-Serra, C. Martí-Gastaldo, J. M. Clemente-Juan, J. Sesé, D. Drung and T. Schuring, *Phys. Rev. B: Condens. Matter Mater. Phys.*, 2010, **82**, 060403.
56 S. Jiang, B. Wang, H. Sun, Z. Wang and S. Gao, *J. Am. Chem. Soc.*, 2011, **133**, 4730.
57 S. Jiang, B. Wang, G. Su, Z. Wang and S. Gao, *Angew. Chem., Int. Ed.*, 2010, **49**, 7448.
58 G. Cucinotta, M. Perfetti, J. Luzon, M. Etienne, P. E. Car, A. Caneschi, G. Calvez, K. Bernot and R. Sessoli, *Angew. Chem., Int. Ed.*, 2012, **51**, 1606.
59 J. D. Rinehart and J. R. Long, *J. Am. Chem. Soc.*, 2009, **131**, 12558.
60 J. D. Rinehart, K. R. Meihaus and J. R. Long, *J. Am. Chem. Soc.*, 2010, **132**, 7572.
61 W. H. Harman, T. D. Harris, D. E. Freedman, H. Fong, A. Chang, J. D. Rinehart, A. Ozarowski, M. T. Sougrati, F. Grandjean, G. J. Long, J. R. Long and C. J. Chang, *J. Am. Chem. Soc.*, 2010, **132**, 18115.
62 J. M. Zadrozny and J. R. Long, *J. Am. Chem. Soc.*, 2011, **133**, 20732.
63 M. A. AlDamen, S. Cardona-Serra, J. M. Clemente-Juan, E. Coronado, A. Gaita-Ariño, C. Martí-Gastaldo, F. Luis and O. Montero, *Inorg. Chem.*, 2009, **48**, 3467.
64 S. Cardona-Serra, J. M. Clemente-Juan, E. Coronado, A. Gaita-Ariño, A. Camón, M. Evangelisti, F. Luis, M. J. Martínez-Pérez and J. Sesé, *J. Am. Chem. Soc.*, DOI: 10.1021/ja305163t.
65 J. J. Baldoví, S. Cardona-Serra, J. M. Clemente-Juan, E. Coronado, A. Gaita-Ariño and A. Palii, *J. Am. Chem. Soc.*, submitted.
66 P. C. E. Stamp and A. Gaita-Ariño, *J. Mater. Chem.*, 2009, **19**, 1718.
67 A. Droghetti and S. Sanvito, *Phys. Rev. Lett.*, 2011, **107**, 047201.
68 A. Palii, B. Tsukerblat, J. M. Clemente-Juan and E. Coronado, *J. Phys. Chem. C*, 2012, **116**, 4999.
69 C. Bosch-Serrano, J. M. Clemente-Juan, E. Coronado, A. Gaita-Ariño, A. Palii and B. Tsukerblat, *ChemPhysChem*, 2012, **13**, 2662.
70 J. Lehmann, A. Gaita-Ariño, E. Coronado and D. Loss, *Nat. Nanotechnol.*, 2007, **2**, 312.
71 J. Lehmann, A. Gaita-Ariño, E. Coronado and D. Loss, *J. Mater. Chem.*, 2009, **19**, 1672.
72 N. Baadji, M. Piacenza, T. Tugsuz, F. Della Sala, G. Maruccio and S. Sanvito, *Nat. Mater.*, 2009, **8**, 813.
73 M. Trif, F. Troiani, D. Stepanenko and D. Loss, *Phys. Rev. Lett.*, 2008, **101**, 217201.
74 L.-H. Bi, U. Kortz, M. H. Dickman, S. Nellutla, N. S. Dalal, B. Keita, L. Nadjo, M. Prinz and M. Neumann, *J. Cluster Sci.*, 2006, **17**, 143.
75 J. M. Clemente-Juan, E. Coronado, A. Gaita-Ariño and N. Suaud, *J. Phys. Chem. A*, 2007, **111**, 9969.
76 M. A. Nielsen and I. L. Chuang, *Quantum Computation and Quantum Information*, Cambridge University, Cambridge, England, 2000.
77 P. C. E. Stamp, *Studies in History and Philosophy of Modern Physics*, 2006, **37**, 467.
78 S. Takahashi, I. S. Tupitsyn, J. van Tol, C. C. Beedle, D. N. Hendrickson and P. C. E. Stamp, *Nature*, 2011, **4**, 76.
79 T. D. Ladd, F. Jelezko, R. Laflamme, Y. Nakamura, C. Monroe and J. L. O'Brien, *Nature*, 2010, **464**, 45.
80 L. M. K. Vandersypen, M. Steffen, G. Breyta, C. S. Yannoni, S. H. Sherwood and I. L. Chuang, *Nature*, 2001, **414**, 883.
81 A. Ardavan and S. J. Blundell, *J. Mater. Chem.*, 2009, **19**, 1754.
82 A. Palii, B. Tsukerblat, J. M. Clemente-Juan, A. Gaita-Ariño and E. Coronado, *Phys. Rev. B: Condens. Matter Mater. Phys.*, 2011, **84**, 184426.
83 A. Ardavan, O. Rival, J. J. L. Morton, S. J. Blundell, A. M. Tyryshkin, G. A. Timco and R. E. P. Winpenny, *Phys. Rev. Lett.*, 2007, **98**, 057201.
84 F. Troiani and M. Affronte, *Chem. Soc. Rev.*, 2011, **40**, 3119.
85 M. N. Leuenberger and D. Loss, *Nature*, 2001, **410**, 789.
86 M. Trif, F. Troiani, D. Stepanenko and D. Loss, *Phys. Rev. Lett.*, 2008, **101**, 217201.
87 M. Trif, F. Troiani, D. Stepanenko and D. Loss, *Phys. Rev. B: Condens. Matter Mater. Phys.*, 2010, **82**, 045429.
88 J. Wesenberg and K. Mølmer, *Phys. Rev. A: At., Mol., Opt. Phys.*, 2003, **68**, 012320.
89 F. Luis, A. Repollés, M. J. Martínez-Pérez, D. Aguilà, O. Roubeau, D. Zueco, P. J. Alonso, M. Evangelisti, A. Camón, J. Sesé, L. A. Barrios and G. Aromí, *Phys. Rev. Lett.*, 2011, **107**, 117203.
90 G. Aromi, D. Aguila, P. Gamez, F. Luis and O. Roubeauc, *Chem. Soc. Rev.*, 2012, **41**, 537.
91 A.-L. Barra, D. Gatteschi, L. Pardi, A. Müller and J. Doring, *J. Am. Chem. Soc.*, 1992, **114**, 8509.
92 S. Bertaina, S. Gambarelli, T. Mitra, B. Tsukerblat, A. Müller and B. Barbara, *Nature*, 2008, **453**, 203.
93 A. Tarantul and B. Tsukerblat, *Inorg. Chim. Acta*, 2010, **363**, 4361.
94 J. Yang, Y. Wang, Z. Wang, X. Rong, C.-K. Duan, J.-H. Su and J. Du, *Phys. Rev. Lett.*, 2012, **108**, 230501.
95 S. Ghosh, S. Datta, L. Friend, S. Cardona-Serra, A. Gaita-Ariño, E. Coronado and S. Hill, *Dalton Trans.*, DOI: 10.1039/C2DT31674A.
96 M. J. Martínez-Pérez, S. Cardona-Serra, C. Schlegel, F. Moro, P. J. Alonso, H. Prima-García, J. M. Clemente-Juan, M. Evangelisti, A. Gaita-Ariño, J. Sesé, J. van Slageren, E. Coronado and F. Luis, *Phys. Rev. Lett.*, 2012, **108**, 247213.

